Registry No. H_2, 1333-74-0; CO, 630-08-0; CO_2, 124-38-9; n-C_6H_{18}, 111-65-9; n-$C_{10}H_{22}$, 124-18-5; n-$C_{12}H_{26}$, 112-40-3; n-$C_{14}H_{30}$, 629-59-4; n-$C_{16}H_{34}$, 544-76-3; n-$C_{20}H_{42}$, 112-95-8.

Literature Cited

(1) Matthews, M. A.; Akgerman, A. *J. Chem. Eng. Data* **1987**, *32*, 317.
(2) Matthews, M. A.; Akgerman, A. *J. Chem. Eng. Data* **1987**, *32*, 319.
(3) Alizadeh, A.; Wakeham, W. A. *Int. J. Thermophys.* **1982**, *3*, 307.
(4) Matthews, M. A.; Akgerman, A. *Int. J. Thermophys.* **1987**, *8*, 363.
(5) Matthews, M. A.; Akgerman, A. *Diffusivities of Synthesis Gas and Fischer-Tropsch Products in Slurry Media*; Quarterly Report, Jan.-Mar. 1986, U. S. Department of Energy DE-AC2284PC 70032.
(6) Matthews, M. A.; Akgerman, A. *AIChE J.* **1987**, *33*, 881.
(7) Matthews, M. A.; Akgerman, A. *J. Chem. Phys.* **1987**, *87*, 2285.
(8) Bondi, A. *J. Phys. Chem.* **1984**, *68*, 441.
(9) *TRC Thermodynamic Tables—Hydrocarbons*; Thermodynamic Research Center, Texas A&M University: College Station, TX, 1986.
(10) Dymond, J. H. *J. Chem. Phys.* **1974**, *60*, 969.

Received for review September 14, 1987. Accepted March 9, 1988. This work was supported by Contract DE-AC22-84PC 70032 from the U.S. Department of Energy.

Nonequilibrium Thermodynamic Studies of Electrokinetic Effects. 20. Electroosmotic Studies of Acetonitrile + Nitromethane Mixtures across a Sintered Disk

R. L. Blokhra,* Satish Kumar, Rajesh Kumar, and Neelam Upadhyay

Department of Chemistry, Himachal Pradesh University, Shimla 171 005, India

Experimental results for electroosmotic velocity and electroosmotic pressure difference for acetonitrile–nitromethane mixtures across a Pyrex sintered disk (G_3) at different compositions, voltages, and temperatures are reported. The results have been interpreted in light of the thermodynamics of irreversible processes. The efficiency of electrokinetic energy conversion (E_e) has also been calculated. The maximum energy conversion took place at half the value of the electroosmotic pressure. The relaxation time τ for all the mixtures has been estimated at different temperatures, and the time dependence of the entropy production has been found to obey Prigogine and Glansdroff's theory of minimum entropy production.

Introduction

Rastogi et al. (*1–5*) and Blokhra et al. (*6–8*) have reported results for electrokinetic effects using a sintered glass disk and a variety of liquids. The workers used the principles of thermodynamics of irreversible process (*9*, *10*) with advantage for treatment of these effects. It was observed earlier that the range of the validity of the theory of thermodynamics of irreversible processes decrease with increase in the dielectric constant (*7*). We have selected an isodielectric mixture of acetonitrile + nitromethane for the present investigation so that there is no variation in the dielectric constant of the liquid phase at different compositions of the constituents of the liquid phase. Further, in our earlier communications (*11*, *12*), we found that acetonitrile is the main contributing component for high electrokinetic energy conversion. The purpose of the present study is to report results of an isodielectric mixture with acetonitrile as one of the constituents so that the role of acetonitrile, if any, could be ascertained in the phenomenon.

Experimental Section

Materials. Acetonitrile (BDH), after keeping over anhydrous calcium oxide for about 48 h, was shaken vigorously with phosphorus pentoxide and was distilled. The first fraction was discarded and the middle fraction was refluxed again over calcium oxide and was refractionated.

Nitromethane (BDH) was first dried by keeping over anhydrous calcium chloride for about 24 h. Then it was purified by simple distillation over fused calcium chloride and was stored in air-tight bottles for the present study.

Results and Discussion

For systems close to equilibrium, the following linear phenomenological relations hold

$$I = L_{11}\Delta\phi + L_{12}\Delta P$$
$$J = L_{21}\Delta\phi + L_{22}\Delta P \qquad (1)$$

where I and J denote the electric current and volume flux, respectively, while $\Delta\phi$ and ΔP are electric potential difference and pressure difference. The phenomenological coefficients L_{11}, L_{12}, L_{21}, and L_{22} relate to electrical conduction, streaming conduction, electroosmosis, and permeation, respectively.

The electroosmotic data have been analyzed as described ealier (*7*). The values of $J_{\Delta P=0}$, $\Delta P_{J=0}$, L_{21}, and L_{22} for different mixtures, 20, 40, 50, 60, and 80% at 298 K and 50% at 303, 308, 313, and 318 K, at different voltages are given in Table I. The volume flow can be written as

$$J_{\Delta P=0} = L_{21}\Delta\phi \qquad (2)$$

Therefore, a plot of $J_{\Delta P=0}$ vs $\Delta\phi$ should give a straight line. Linear relationship between J and $\Delta\phi$ has been found for all the mixtures studied at all temperatures. This linear relationship holds good for voltages between 40 and 260 V. A sample plot of $J_{\Delta P=0}$ vs $\Delta\phi$ (for 40% acetonitrile at 298 K) is shown in Figure 1.

Efficiency of Energy Conversion

Osterle and co-workers (*13–15*), and Kedam and Caplan (*16*), have discussed the efficiency of electrokinetic energy conversion on the basis of nonequilibrium thermodynamics. The phenomenon of electroosmosis flow can be used with advantage in the design of energy conversion devices. In this case, electrical energy is converted into mechanical work.

In general the equation for conversion efficiency E_e, in terms of conjugate fluxes and forces J and X, has been deduced by Osterle as

$$E_e = -\frac{J_o X_o}{J_i X_i} \qquad (3)$$

where subscripts o and i represent the output and input quantities, respectively. The negative sign in eq 3 indicates that

0021-9568/88/1733-0347$01.50/0

Table I. Electroosmotic Data for Different Acetonitrile + Nitromethane Mixtures at 298 K and for 50% Acetonitrile at Different Temperatures

$\Delta\phi$, V	$J_{\Delta P=0} \times 10^5$, ms^{-1}	$\Delta P_{J=0} \times 10^{-1}$, $N\ m^{-2}$	$L_{22} \times 10^6$, $m^3\ N^{-1}\ s^{-1}$	$L_{21} \times 10^6$, $m\ A\ J^{-1}$	$\Delta\phi$, V	$J_{\Delta P=0} \times 10^5$, ms^{-1}	$\Delta P_{J=0} \times 10^{-1}$, $N\ m^{-2}$	$L_{22} \times 10^6$, $m^3\ N^{-1}\ s^{-1}$	$L_{21} \times 10^6$, $m\ A\ J^{-1}$
				20% CH_3CN					
40	5.0	2.431	1.2	2.06	160	20.0	12.529	1.2	1.60
60	6.9	3.179	1.2	2.17	180	22.8	13.370	1.2	1.71
80	9.4	4.114	1.2	2.28	200	25.0	17.578	1.2	1.42
100	12.5	6.919	1.2	1.81	220	26.8	19.168	1.2	1.40
120	14.4	10.285	1.2	1.40	240	29.2	20.477	1.2	1.43
140	17.5	11.687	1.2	1.50	260	32.5	21.318	1.2	1.52
				40% CH_3CN					
40	7.0	2.191	1.7	3.19	160	25.9	11.139	1.6	2.33
60	9.9	3.469	1.6	2.85	180	28.9	12.052	1.6	2.40
80	12.0	4.747	1.6	2.53	200	32.0	17.713	1.6	2.81
100	16.0	6.756	1.6	2.37	220	34.9		1.6	1.37
120	18.9	8.948	1.6	2.11	240	38.8		1.6	1.38
140	22.9	9.678	1.6	2.37	260	41.8		1.6	1.42
				50% CH_3CN					
40	6.0	3.698	1.5	1.62	180	26.0	15.335	1.4	1.70
60	8.5	3.798	1.4	2.24	200	28.5	15.516	1.4	1.84
80	11.5	6.856	1.4	1.68	220	31.5	15.877	1.4	1.98
120	17.5	8.479	1.4	2.06	240	34.5	16.418	1.4	2.10
140	20.0	11.186	1.4	1.79	260	37.5	19.846	1.4	1.89
160	23.0	14.975	1.4	1.54					
				60% CH_3CN					
40	9.0	4.007	2.3	2.25	160	36.0	16.926	2.3	2.15
60	13.9	8.014	2.3	1.73	180	41.9	18.294	2.3	2.28
80	18.0	9.234	2.3	1.95	200	46.0	19.950	2.3	2.31
100	23.0	10.628	2.3	2.16	220	50.8	24.044	2.3	2.11
120	27.0	12.719	2.3	2.12	240	54.9	27.529	2.3	1.99
140	31.9	15.507	2.3	2.06	260	59.8	29.446	2.3	2.03
				80% CH_3CN					
40	12.0	3.415	3.0	3.57	160	46.4	16.396	2.9	2.83
60	18.0	7.301	3.0	2.50	180	51.8	17.079	2.9	3.03
80	24.0	7.515	2.9	3.20	200	58.0	23.228	2.9	2.50
100	29.0	7.771	2.9	3.73	220	63.8	28.096	2.9	2.27
120	35.0	9.906	2.9	3.53	240	68.8	29.804	2.9	2.31
140	41.0	11.785	2.9	3.48	260	75.9	28.865	2.9	2.63
				50% CH_3CN at 303 K					
40	6.0	4.306	1.50	1.39	160	23.5	16.417	1.46	1.43
60	9.0	7.266	1.50	1.24	180	26.5	16.865	1.47	1.57
80	11.5	8.702	1.43	1.32	200	29.5	22.428	1.47	1.32
100	18.0	11.662	1.50	1.29	220	32.5	23.504	1.47	1.38
120	17.5	12.200	1.45	1.43	240	35.5	24.042	1.47	1.48
140	20.5	13.367	1.46	1.53	260	38.5	24.311	1.48	1.58
				50% CH_3CN at 308 K					
40	6.5	3.925	1.62	1.66	160	25.5	14.809	1.59	1.72
60	9.5	4.282	1.58	2.22	180	28.5	15.523	1.58	1.84
80	13.5	7.137	1.68	1.89	200	31.5	16.058	1.57	1.96
100	16.0	8.921	1.60	1.79	220	35.0	17.218	1.59	2.03
120	19.0	9.278	1.58	2.05	240	38.0	18.734	1.58	2.03
140	22.0	12.846	1.57	1.71	260	41.0	19.448	1.57	2.11
				50% CH_3CN at 313 K					
40	7.5	2.663	1.87	2.82	160	29.0	12.784	1.81	2.42
60	11.0	3.018	1.83	3.64	180	32.5	13.405	1.80	2.47
80	14.5	5.149	1.81	2.82	200	36.0	14.559	1.80	
100	18.0	6.835	1.80	2.63	220	39.5	15.092	1.79	2.65
120	21.5	8.167	1.79	2.51	240	43.0	15.624	1.79	2.75
140	25.0	9.943	1.79	2.27	260	47.0	15.980	1.80	2.94
				50% CH_3CN at 318 K					
40	6.5	3.710	1.62	1.75	160	27.0	12.545	1.68	2.15
60	10.0	4.240	1.60	2.36	180	30.0	12.987	1.66	2.31
80	13.0	7.863	1.62	1.65	200	33.5	14.489	1.67	2.31
100	16.5	7.951	1.65	2.08	220	37.0	15.196	1.68	2.43
120	20.0	10.248	1.66	1.95	240	40.0	15.549	1.66	2.57
140	23.5	11.308	1.67	2.08	260	43.5	16.344	1.67	2.66

output forces and fluxes are in a direction opposite to that of input forces and fluxes. In the case of electroosmosis, the applied electrical potential difference $\Delta\phi$ is the input force and the consequent pressure difference ΔP is the output force. Therefore, the expression for the energy conversion efficiency, E_e, for electroosmosis in the range of linear phenomenological laws is given by

$$E_e = -\frac{J\Delta P}{(\Delta\phi)^2/R} \tag{4}$$

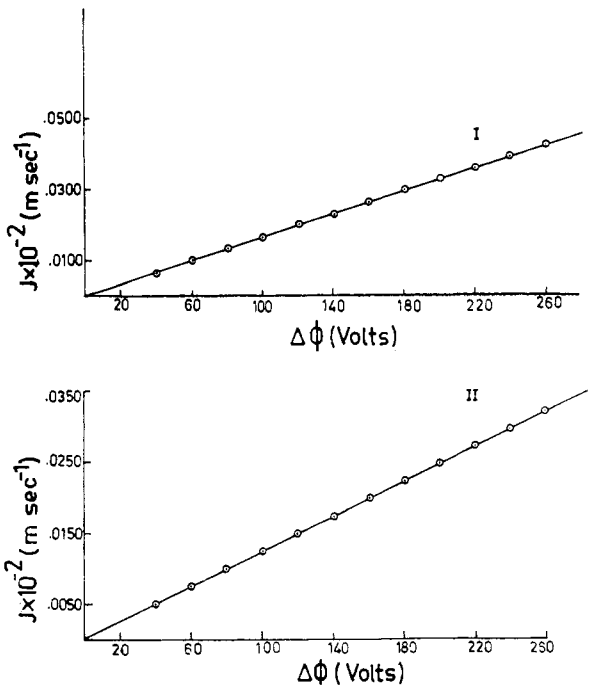

Figure 1. Variation of $J_{\Delta P=0}$ with $\Delta\phi$: I, 40% ACN–CH_3NO_2; II, 20% ACN–CH_3NO_2.

Table II. Values of $E_{e\,max}$ for Different Compositions of Acetonitrile + Nitromethane at Different Temperatures

temp, K	% composn CH_3CN	$E_{m\,max} \times 10^6$	$\Delta P \times 10^{-1}$, N m^{-2}
298	20	1.7	3.30
298	40	2.6	3.50
298	60	3.8	5.30
298	80	3.5	3.75
298	50	1.6	3.40
303	50	3.1	5.60
308	50	2.4	4.50
313	50	2.0	3.50
318	50	2.10	3.75

where R is the electric resistance of the total system.

In the case of electroosmosis, the volume flow J vanishes when the steady state is reached so that ΔP equals the electroosmotic pressure. This means that E_e will be zero either if ΔP equals the electroosmotic pressure or if $\Delta P = 0$. Therefore, the plot of E_e vs ΔP for a fixed value of electric potential difference $\Delta\phi$ must pass through a maximum. This has been found to be so in all the cases at 100 V. This is shown in Figure 2. It has been found that E_e attains maximum value when ΔP equals half the values of electroosmotic pressure difference; i.e.

$$\Delta P = -\tfrac{1}{2}\Delta P_{J=0} \tag{5}$$

The value of $E_{e\,max}$ from such plots is recorded in Table II. Table II shows that the value of $E_{e\,max}$ in the present case is much lower than that of acetonitrile + DMF mixtures and ethylene glycol + acetonitrile + DMF (*11*). This lower value of $E_{e\,max}$ in this case may be attributed to strong interaction between the molecules of the mixture, and the higher value of $E_{e\,max}$ for acetonitrile + DMF and ethylene glycol + acetonitrile + DMF mixtures is not characteristic of acetonitrile.

Relaxation Time of Electroosmotic Flow. The relaxation time, τ, for electroosmosis is defined (*17*) as

$$\tau = q^0\delta/2q\rho g\beta \tag{6}$$

where ρ is the density of liquid, g the gravitational acceleration, q the cross section area of the diaphragm, δ the thickness of

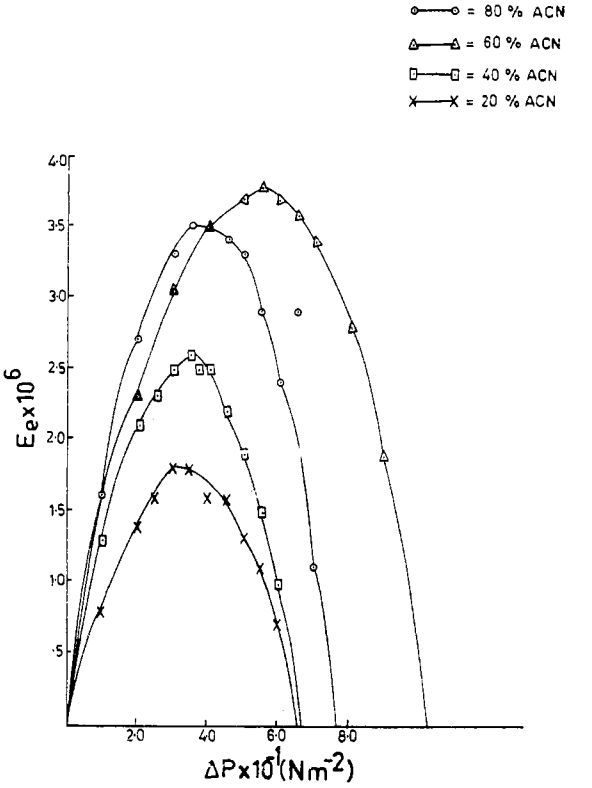

Figure 2. Plot of E_e vs ΔP for different compositions at 100 V and 25 °C.

Table III. Relaxation Time (τ) for Electroosmotic Flow with Acetonitrile + Nitromethane Mixtures at Different Temperatures

temp, K	% compn CH_3CN	τ, s	temp, K	% compn CH_3CN	τ, s
298	20	6.55	303	50	5.57
298	40	5.18	308	50	5.89
298	60	7.35	313	50	5.23
298	80	9.9	318	50	9.21
298	50	7.67			

diaphragm, β the permeability, and q^0 the cross section of the capillary tube in which the liquid rises during electroosmotic flow. Using eq 6, it has been deduced that the change in the height of the liquid column with time in the vertical tube is given by

$$dh/dt = (h_\infty - h)/\tau \tag{7}$$

where h_∞ is the height level corresponding to the steady state of electroosmotic pressure and h is height at time t. Integrating eq 7, and taking account of the initial condition $h = h_0$, for $t = 0$, we have

$$\log (h_\infty - h_0)/(h_\infty - h) = t/\tau \tag{8}$$

From eq 8, τ can be estimated from the slope of linear plots of log $(h_\infty - h)$ vs t. The values of τ obtained are given in Table III.

Entropy Production in Electroosmosis. Hasse (*18*) dealt with the time dependence of the dissipation function/entropy production in electroosmosis experiments in a system approaching a steady state. In the case of steady-state condition, the pressure difference ΔP and electrical potential difference $\Delta\phi$ no longer depend on time. Further it has been observed that J and $d(\Delta P)/dt$ have opposite signs (*17*, *19*), except in stationary states where both quantities vanish.

Thus we have

$$J\Delta^*P \leq 0 \quad \text{or} \quad -J\Delta^*P \geq 0 \tag{9}$$

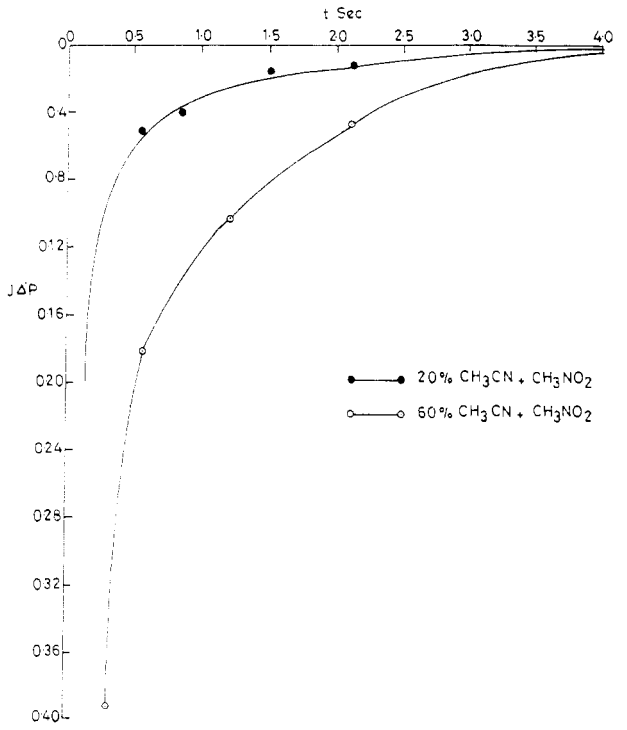

Figure 3. Plot of $J\Delta^{\bullet}P$ vs time.

The equality sign applies to steady state. Now, according to the generalization (*20*), we have

$$m = -(I\Delta^{\bullet}\phi + J\Delta^{\bullet}P) \geq 0 \qquad (10)$$

Here the quantity $J\Delta^{\bullet}P$ is that part of the rate of increase of dissipation function (*11*) which is due to change of the forces for the fixed values of the fluxes. According to the evolution criterion, the quantity is negative or zero (steady state) for any distance from equilibrium, provided the temperature is kept constant. The above conditions were maintained (approximately) as the electrical potential difference is fixed and the total system is closed. Thus eq 10 can be reduced to eq 9, because $\Delta\phi$ is kept constant is these experiments. J and $\Delta^{\bullet}P$ were evaluated from the slope of the curve obtained by plotting the riss of liquid against time, i.e., approach to steady state which was determined experimentally. In Figure 3 the values of $-J\Delta^{\bullet}P$ for 20% and 60% acetonitrile + nitromethane mixtures are plotted at different intervals of time.

The curve approaches the time axis asymptotically, proving the theorem in the case of electroosmosis, and also it gives the evaluation of entropy production. Similar plots have been obtained in the case of the other compositions of the mixtures.

Registry No. CH_3CN, 75-05-8; nitromethane, 75-52-5.

Literature Cited

(1) Rastogi, R. P.; Jha, K. M. *Trans. Faraday Soc.* **1966**, *62*, 585.
(2) Rastogi, R. P.; Jha, K. M. *J. Phys. Chem.* **1966**, *70*, 1017.
(3) Rastogi, R. P.; Singh, K.; Srivastava, M. L. *J. Phys. Chem.* **1969**, *73*, 46.
(4) Rastogi, R. P.; Singh, K.; Singh, S. N. *J. Phys. Chem.* **1969**, *73*, 1593.
(5) Rastogi, R. P.; Srivastava, M. L.; Singh, S. N. *J. Phys. Chem.* **1970**, *74*, 2960.
(6) Blokhra, R. L.; Singal, T. C. *Indian. J. Chem.* **1975**, *13*, 913.
(7) Blokhra, R. L.; Parmar, M. L.; Sharma, V. P. *Colloid Interface Science*; Kerkar, M., Ed.; Academic: New York, 1976; Vol. IV, p259.
(8) Blokhra, R. L.; Parmar, M. L. *Indian J. Chem.* **1977**, *15A*, 384.
(9) Hasse, R. *Thermodynamics of Irreversible Processes*; Addison-Wasley: Reading, MA, 1969.
(10) Prigogine, I. *Introduction to Thermodynamics of Irreversible Process*; Wiley: New York, 1967.
(11) Blokhra, R. L.; Parmar, M. L.; Agarwal, S. K. *J. Electroanal. Chem.* **1976**, *89*, 417.
(12) Blokhra, R. L.; Agarwal, S. K.; Arora, Neerja *J. Colloid Interface Sci.* **1980**, *73*, 88.
(13) Osterle, J. F. *J. Appl. Mech.* **1964**, *31*, 161.
(14) Osterle, J. F. *Appl. Sci. Res.* **1964**, *12*, 425.
(15) Morrison, F. A.; Osterle, J. F. *J. Chem. Phys.* **1965**, *43*, 211.
(16) Kedam, O.; Caplan, S. R. *Trans. Faraday Soc.* **1965**, *61*, 1897.
(17) Hasse, R. *Z. Phys. Chem. N.F.* **1976**, *103*, 235.
(18) Hasse, R. *Z. Phys. Chem. N.F.* **1976**, *103*, 247.
(19) Srivastava, R. C.; Blokhra, R. L. *Indian J. Chem.* **1963**, *1*, 156.
(20) Glansdroff, P.; Prigogine, I. *Physica,'s Grav.* **1954**, *20*, 773.

Received for review September 17, 1987. Accepted March 15, 1988.

Partial Miscibility Behavior of the Ethane + Propane + *n*-Dotriacontane Mixture

Susana S. Estrera and Kraemer D. Luks*

Department of Chemical Engineering, University of Tulsa, Tulsa, Oklahoma 74104-3189

The liquid–liquid–vapor partial miscibility of the mixture ethane + propane + *n*-dotriacontane is experimentally studied by using a visual cell (stoichiometric) technique. The ternary mixture, which has no constituent binary partial miscibility, has a liquid–liquid–vapor region bounded by upper and lower critical end point loci and a quadruple point locus (solid–liquid–liquid–vapor). The three-phase region extends from about 47 to 95 °C at pressures from 41 to 52 bar. The boundaries of the three-phase region are located in pressure–temperature space, and phase compositions and molar volumes of the three fluid phases are reported along isotherms at 50, 60, and 70 °C.

Introduction

The authors have undertaken an extensive study of phase equilibria behavior and liquid–liquid–vapor (LLV) immiscibility phenomena in prototype rich gas + oil mixtures. "Rich gas", a mixture of methane + ethane + propane that has been separated from a live oil, is sometimes reinjected into reservoirs to enhance the recovery of the remaining oil. The purposes of the study are to map out the patterns of multiphase equilibria of these prototype mixtures in thermodynamic phase space and to generate a phase equilibria data base that would be useful for developing and testing equation-of-state models used to predict phase equilibria in and near regions of LLV immiscibility.

There is only limited immiscibility in binary mixtures of *n*-paraffins + methane, ethane, or propane. Partial miscibility has been observed in the mixtures methane + *n*-hexane (*1*) and methane + *n*-heptane (*2*, *3*). *n*-Pentane is completely miscible with methane, while *n*-octane and higher members of the homologous series of *n*-paraffins are too molecularly dissimilar to methane to have a LLV region. Instead, a solid phase of the *n*-paraffin forms, creating two separate LV regions. The thermodynamic phase space topography of systems exhibiting

0021-9568/88/1733-0350$01.50/0